

Droplet epitaxial growth of highly symmetric quantum dots emitting at telecommunication wavelengths on InP(111)A

Neul Ha, Xiangming Liu, Takaaki Mano, Takashi Kuroda, Kazutaka Mitsuishi, Andrea Castellano, Stefano Sanguinetti, Takeshi Noda, Yoshiki Sakuma, and Kazuaki Sakoda

Citation: *Applied Physics Letters* **104**, 143106 (2014); doi: 10.1063/1.4870839

View online: <http://dx.doi.org/10.1063/1.4870839>

View Table of Contents: <http://scitation.aip.org/content/aip/journal/apl/104/14?ver=pdfcov>

Published by the [AIP Publishing](#)

Articles you may be interested in

[Elemental diffusion during the droplet epitaxy growth of In\(Ga\)As/GaAs\(001\) quantum dots by metal-organic chemical vapor deposition](#)

Appl. Phys. Lett. **104**, 022108 (2014); 10.1063/1.4859915

[Room temperature magnetoelectric properties of type-II InAsSbP quantum dots and nanorings](#)

Appl. Phys. Lett. **100**, 033104 (2012); 10.1063/1.3676437

[Quantitative investigations of optical absorption in InAs/InP \(311\) B quantum dots emitting at 1.55 \$\mu\$ m wavelength](#)

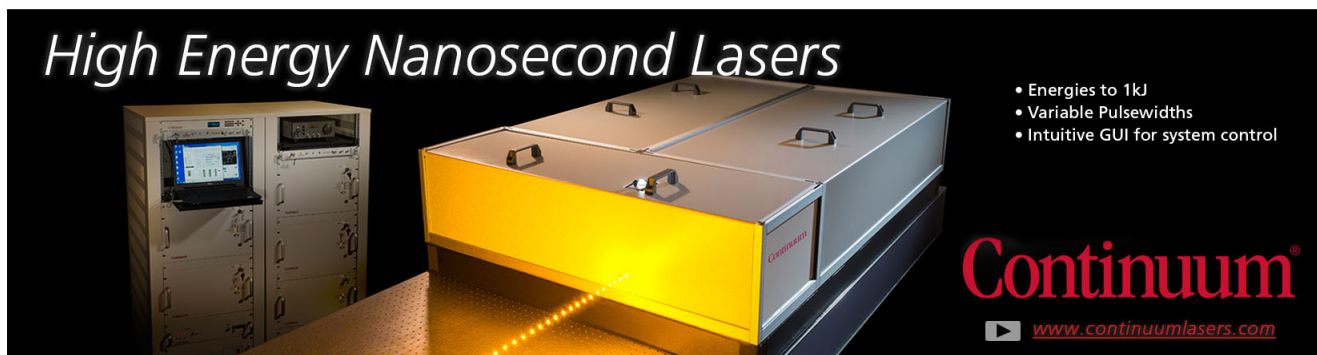
Appl. Phys. Lett. **85**, 5685 (2004); 10.1063/1.1832750

[InAs/InP quantum dots emitting in the 1.55 \$\mu\$ m wavelength region by inserting submonolayer GaP interlayers](#)

Appl. Phys. Lett. **85**, 1404 (2004); 10.1063/1.1785859

[Midinfrared photoluminescence of InAsSb quantum dots grown by liquid phase epitaxy](#)

Appl. Phys. Lett. **77**, 3791 (2000); 10.1063/1.1329168

The advertisement features a black background with the text 'High Energy Nanosecond Lasers' in a white, italicized serif font at the top left. Below the text, there is a photograph of a large, industrial-grade laser system with a prominent yellow glow from its front panel. To the right of the image, a list of features is provided in white text: 'Energies to 1kJ', 'Variable Pulsewidths', and 'Intuitive GUI for system control'. At the bottom right, the 'Continuum' logo is displayed in a red, serif font, with the website address 'www.continuumlasers.com' and a small play button icon below it.

Droplet epitaxial growth of highly symmetric quantum dots emitting at telecommunication wavelengths on InP(111)A

Neul Ha,^{1,2} Xiangming Liu,¹ Takaaki Mano,^{1,a)} Takashi Kuroda,^{1,2} Kazutaka Mitsuishi,¹ Andrea Castellano,^{1,3} Stefano Sanguinetti,³ Takeshi Noda,¹ Yoshiki Sakuma,¹ and Kazuaki Sakoda¹

¹National Institute for Materials Science, 1-2-1 Sengen, Tsukuba 305-0047, Japan

²Graduate School of Engineering, Kyushu University, NIMS, Tsukuba 305-0044, Japan

³Dip. di Scienza dei Materiali, Università di Milano Bicocca, Via Cozzi 55, I-20125 Milano, Italy

(Received 2 February 2014; accepted 28 March 2014; published online 8 April 2014)

We demonstrate the formation of InAs quantum dots (QDs) on InAlAs/InP(111)A by means of droplet epitaxy. The C_{3v} symmetry of the (111)A substrate enabled us to realize highly symmetric QDs that are free from lateral elongations. The QDs exhibit a disk-like truncated shape with an atomically flat top surface. Photoluminescence signals show broad-band spectra at telecommunication wavelengths of 1.3 and 1.5 μm . Strong luminescence signals are retained up to room temperature. Thus, our QDs are potentially useful for realizing an entangled photon-pair source that is compatible with current telecommunication fiber networks. © 2014 AIP Publishing LLC. [<http://dx.doi.org/10.1063/1.4870839>]

Quantum dots (QDs) are promising candidates for on-demand entangled photon emitters.^{1–6} A single QD emits a pair of photons associated with the transition cascade from the biexciton-state to the exciton-state, and subsequently to the ground state. This transition has two paths depending on the exciton angular momentum. When these two paths are degenerate and are energetically indistinguishable, two photons emitted along the cascade become entangled on a polarization basis. In conventional QDs grown on a cubic semiconductor along the [100] crystal axis, symmetry breaking occurs owing to the C_{2v} symmetry of the semiconductor surfaces.^{7–10} To circumvent symmetry breaking, QDs formed along the [111] crystal axis with C_{3v} symmetry are promising. However, self-assembled QDs cannot be formed on the {111} surfaces by means of conventional Stranski–Krastanov (SK) mode (i.e., two-dimensional growth followed by island formation).¹¹ On these surfaces, dislocations form at the interfaces preferentially in order to relax strain.^{12,13} Therefore, other techniques, such as droplet epitaxy and pyramidal site control, have been used to create symmetric QDs in InGaAs/GaAs, GaAs/AlGaAs, and InGaAsN/GaAs systems.^{14–16} Entangled photons at wavelengths near 850 nm have been observed in pyramidal QDs.¹⁷ Moreover, we have recently demonstrated filtering-free violation of Bell's inequality using self-assembled QDs grown on GaAs(111)A by droplet epitaxy.¹⁸

Extension of the emission wavelengths of these symmetric QDs into the optical fiber telecommunication wavelength ranges of 1.3 and 1.5 μm is highly desired. To achieve such extension, the use of InAs QDs on InP substrates is suitable^{19–21} because highly strained InAs QDs formed on GaAs typically emit photons at the wavelengths of less than 1 μm .^{3,8,9,11,15}

In this study, we investigated the droplet epitaxy of InAs QDs on InAlAs/InP(111)A. Owing to the three-fold rotational symmetry of the growth plane, highly symmetric InAs

QDs were realized. Efficient photoluminescence (PL) emissions from the QDs at both 1.3 and 1.5 μm were realized at temperatures up to room temperature.

Samples were grown on semi-insulating (Fe-doped) InP(111)A substrates using a solid-source molecular beam epitaxy. After the growth of an $\text{In}_{0.52}\text{Al}_{0.48}\text{As}$ buffer layer of 150-nm thickness at 470 °C, we supplied 0.8 monolayers (ML) or 1.6 ML of indium with a flux of 0.2 ML/s at 270 °C. The supply of indium *without* As_4 enabled the formation of liquid indium droplets, which were confirmed by observation of a halo pattern in reflection high-energy electron diffraction (RHEED) measurements.¹⁴ Next, we supplied an As_4 flux of 3×10^{-5} Torr at 270 °C, which led the RHEED pattern to change from halo to spotty due to the crystallization of indium droplets into InAs QDs.¹⁴ After annealing at 370 °C for 5 min under As_4 supply,²² InAs QDs were capped with an $\text{In}_{0.52}\text{Al}_{0.48}\text{As}$ layer of 75-nm thickness at 370 °C. The samples were then annealed at 470 °C for 5 min for improving crystal quality.

The surface morphology of uncapped QDs was studied by atomic force microscope (AFM). The morphology of capped QDs was studied by cross-sectional transmission electron microscopy (X-TEM) in annular dark field-scanning transmission electron microscopy (ADF-STEM) mode. PL spectra were measured at 9 K using the 532-nm line of a continuous-wave diode-pumped laser. The PL signals were dispersed by a polychromator with a focal length of 50 cm and were detected by a cooled InGaAs photodiode array or a Si charge-coupled device camera.

Figures 1(a) and 1(b) show AFM images of the samples grown with an indium supply of 0.8 and 1.6 ML, respectively, after crystallization at 270 °C. The images reveal well-defined QDs with a density of (a) $1.1 \times 10^{11} \text{ cm}^{-2}$ and (b) $5.4 \times 10^{10} \text{ cm}^{-2}$. Thus, with increasing indium, the QD density decreases roughly by a factor of two. In parallel, the average size of QDs increases from 18 nm to 30 nm in base diameter and from 0.83 to 1.6 nm in height. These changes in QD size and density imply that coalescence and/or

^{a)} Author to whom correspondence should be addressed. Electronic mail: mano.takaaki@nims.go.jp

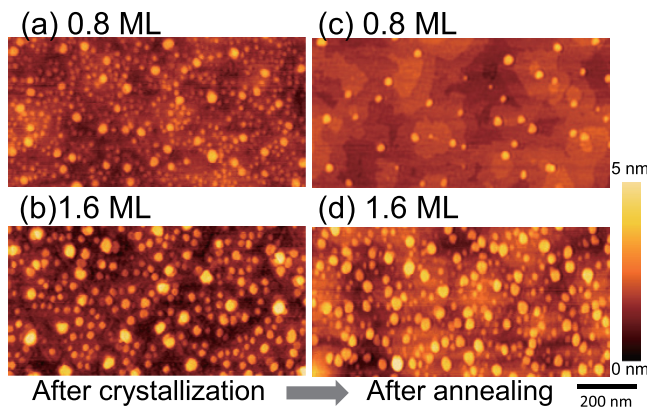


FIG. 1. AFM images of (a) 0.8 and (b) 1.6 ML InAs QDs on InAlAs after crystallization at 270 °C (left). (c) and (d) AFM images after annealing at 370 °C (right).

ripening of the small indium droplets occurred with increasing indium supply.²³ Notably, QDs were formed even when the indium supply was less than 1 ML, suggesting that the droplet nucleation occurred immediately after supplying indium on the surface (without forming a two-dimensional layer).¹⁶ This immediate nucleation of droplets is likely facilitated by the absence of any excess As atoms on the (111)A-(2 × 2) surface, as has been reported for GaAs surfaces.²⁴

Figures 1(c) and 1(d) show AFM images of a surface after annealing at 370 °C for samples with an indium of 0.8 and 1.6 ML, respectively. QDs are still visible even after annealing. For the 0.8 ML indium sample, however, the QD density was found to decrease drastically after annealing to $8.8 \times 10^9 \text{ cm}^{-2}$ (Fig. 1(c)). In contrast, for the 1.6 ML indium sample, the density remained almost unchanged at $5.4 \times 10^{10} \text{ cm}^{-2}$ (Fig. 1(d)).

The impact of annealing on the surface morphology is further depicted in the size distribution of QDs in Fig. 2. Here, we analyzed the QD volume with the assumption that each QD had a hemispherical shape for simplicity. For the 0.8 ML indium sample (Fig. 2(a)), more than 80% of QDs exhibit a volume lower than 150 nm^3 (highlighted by the broken line) after crystallization (before annealing). However, these small QDs mostly disappear in the sample

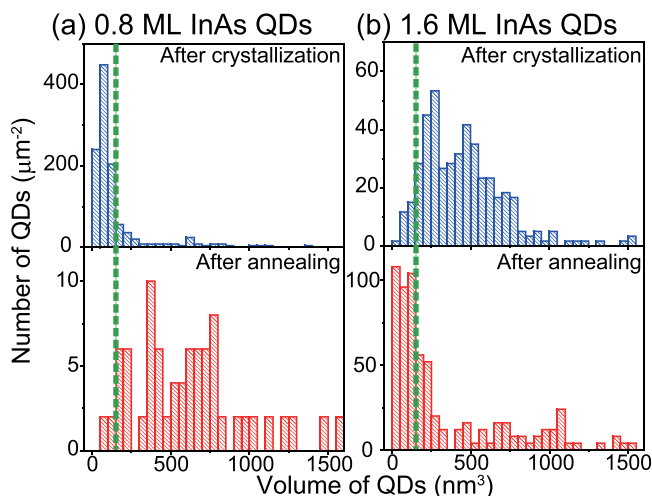


FIG. 2. Histograms of QD volume for (a) 0.8 and (b) 1.6 ML InAs after crystallization at 270 °C and after annealing at 370 °C. They are plotted with a volume bin of 50 nm^3 .

after annealing, which leads to the observation of a decrease in the QD density. For the 1.6 ML indium sample (Fig. 2(b)), the QD volume is distributed around an average value of 740 nm^3 before annealing, and around 350 nm^3 after annealing.

Thus, for both samples, the average volume was significantly reduced by annealing. For the 0.8 ML sample, this volume reduction resulted in a significant density reduction since most of the QDs were already of low volume before annealing.

We attribute this annealing-induced volume reduction to the growth of a two-dimensional layer caused by diffusion of atoms from InAs QDs. In the case of droplet epitaxy, QDs are grown by a kinetically limited processes without forming a two-dimensional layer. At the annealing step, however, some amount of InAs flows out from the QDs and forms a two-dimensional layer, which might reduce the local strain energy in the vicinity of the QDs. This emergence of a two-dimensional layer following the QD formation is in the reverse order of SK growth, for which a two-dimensional layer (i.e., a wetting layer) appears before QDs.

The presence of a two-dimensional layer was confirmed by the X-TEM image of the 1.6 ML QDs embedded in the InAlAs barrier in Fig. 3(a). A two-dimensional layer with a thickness of around 1 ML is clearly visible, as indicated with an arrow. The buried QD shows a truncated disk-like shape with an atomically smoothed surface on the top. No dislocation was found at the interface between the QD and the InAlAs barrier, indicating the high crystalline quality of the present samples. The clear contrast between the QD and the InAlAs barrier evidences the formation of abrupt interface. The formation of disk-like QDs with flat surfaces has been also observed in droplet epitaxial GaAs QDs formed on an AlGaAs (111)A surface.¹⁶

Figure 3(b) shows the three-dimensional view of an AFM image of uncapped InAs QDs grown with 1.6 ML indium. Despite a finite spatial resolution, the flat-top shape is

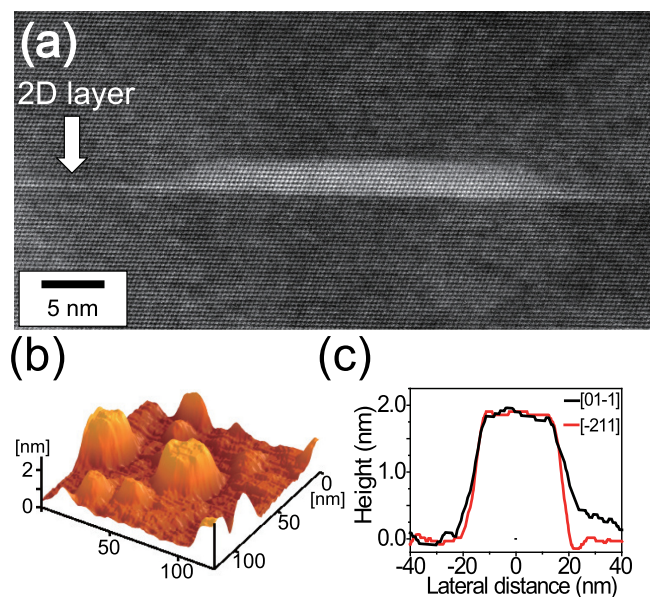


FIG. 3. (a) X-TEM image of 1.6 ML QDs after capping. The white arrow indicates the two-dimensional layer. (b) Three-dimensional view of AFM image of InAs QDs after annealing. (c) Cross-sectional profiles of a QDs along the $[-211]$ and $[01-1]$ directions after annealing at 370 °C.

clearly visible for relatively large QDs. Figure 3(c) shows typical cross-sectional profiles obtained along two orthogonal directions ($[-211]$ and $[01-1]$) of a QD shown in Fig. 3(b). The profiles are nearly identical. This isotropic feature is a direct consequence of the three-fold rotational symmetry of the (111)A surface,²⁴ on which equivalent directions appear with respect to every 120° rotation. As a consequence of this symmetry, in-plane anisotropy is eliminated in QDs on (111)A surfaces.

Figures 4(a) and 4(b) show the PL spectra of ensembles of QDs prepared with 0.8 and 1.6 ML indium, respectively. At short wavelengths, emission from the two-dimensional layer was observed around 840 nm, together with emissions from the InP substrate at 875 and 900 nm and the InAlAs barrier at ~ 800 nm. The two-dimensional layer signal is relatively higher for the 0.8 ML sample than for the 1.6 ML sample due to differences in the QD density, as shown in Figs. 1(c) and 1(d).

At long wavelengths, high-yield QD emissions were observed in both samples at a wide spectral range of 950–1600 nm at 9 K. This broad-band emission is consistent with a large size distribution of QDs observed by AFM. The PL spectrum consists of multiple peaks, rather than a broad single peak. The relative intensity between the multiple peaks was independent of excitation intensity (data not shown). Thus, the observed spectral multiplet is ascribed to different families of QDs whose heights vary by a monolayer step.^{16,19} The split multiple peaks indicate that the QDs have a truncated shape with a flat top, as shown in Fig. 3. AFM measurements indicate that the average height of QDs prepared with an indium supply of 0.8 ML is 1.6 nm, which corresponds to 5 ML InAs.

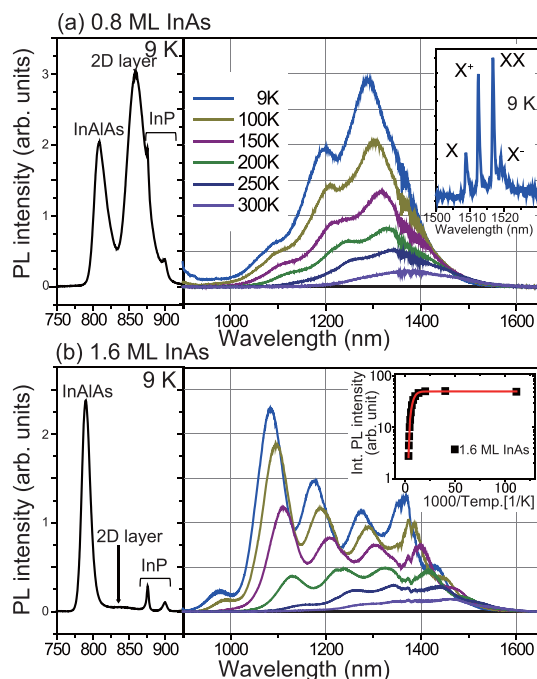


FIG. 4. Temperature dependent PL spectra of (a) 0.8 ML and (b) 1.6 ML QDs (right) and PL spectra near 800 nm at 9 K (left). The inset of (a) shows the μ PL spectrum of a single QD emitting at $1.5 \mu\text{m}$. The inset of (b) shows integrated PL intensity of 1.6 ML QDs as a function of inverse temperature. The red line corresponds to the fit curve.

With increasing temperature, the multiple peaks shift to longer wavelengths in unison. Even at 300 K, the PL signal remains, although its intensity is 1/10 of that observed at 9 K. The integrated PL intensity change as a function of the temperature was well reproduced by the Arrhenius-type equation^{25,26} using two activation energies of 160 meV and 36 meV, as shown in inset of Fig. 4(b). These higher (160 meV) and lower (36 meV) activation energies might be related to the carrier escape from the QDs and nonradiative scattering in the barrier, respectively.^{26,27} The observed room temperature PL emissions reflect the high crystal quality and strong confinement in this QD system.

The inset of Fig. 4(a) shows a typical micro-PL (μ PL) spectrum of an isolated single QD, which emits at a wavelength of around $1.5 \mu\text{m}$.²⁸ Bright emission from the single QD is visible and it consists of four sharp lines, which are identified from the shortest to longest wavelengths as neutral excitons (X), positively charged excitons (X^+), neutral biexcitons (XX), and negatively charged excitons (X^-), respectively. These lines were assigned by careful analysis of the excitation power dependence and linear and circular polarization characteristics.²⁹ For some QDs, we observed significant line broadening with an FWHM as large as $\sim 300 \mu\text{eV}$, which is due to spectral diffusions caused by random charge trapping in the vicinity of QDs.³⁰ The observed excitonic features are of importance for the application of our QD systems to single-photon and entangled photon-pair sources.

In conclusion, we demonstrated the formation of InAs QDs on InAlAs/InP(111)A substrates by means of droplet epitaxy. AFM and X-TEM images reveal that symmetric QDs with flat tops were formed. During the annealing of QDs, a two-dimensional layer was formed by flowing out of InAs from the QDs. High-yield PL emission was observed from the QDs up to room temperature, indicating high QD quality. In μ PL, bright excitonic emission from the single QDs was observed. Using droplet epitaxy, we can easily tune the size and density of the QDs during the droplet formation process. Therefore, we believe that the present system is highly promising to realize on-demand entangled photon emission at telecommunication wavelengths.

We acknowledge B. Urbaszek, H. Nakajima, H. Kumano, and I. Suemune for fruitful discussions. This work was partially supported by a Grant-in-Aid for Scientific Research (C), No. 2539011.

¹Y. Arakawa and H. Sakaki, *Appl. Phys. Lett.* **40**, 939 (1982).

²O. Benson, C. Santori, M. Pelton, and Y. Yamamoto, *Phys. Rev. Lett.* **84**, 2513 (2000).

³R. M. Stevenson, R. J. Young, P. Atkinson, K. Cooper, D. A. Ritchie, and A. J. Shields, *Nature (London)* **439**, 179 (2006).

⁴M. Akopian, N. H. Lindner, E. Poem, Y. Berlatzky, J. Avron, D. Gershoni, B. D. Gerardot, and P. M. Petroff, *Phys. Rev. Lett.* **96**, 130501 (2006).

⁵A. Muller, W. Fang, J. Lawall, and G. S. Solomon, *Phys. Rev. Lett.* **103**, 217402 (2009).

⁶A. Dousse, J. Suffczynski, A. Beveratos, O. Krebs, A. Lemaitre, I. Sagnes, J. Bloch, P. Voisin, and P. Senellart, *Nature (London)* **466**, 217 (2010).

⁷D. Gammon, E. S. Snow, B. V. Shanabrook, D. S. Katzer, and D. Park, *Science* **273**, 87 (1996).

⁸M. Bayer, A. Kuther, A. Forchel, A. Gorbunov, V. B. Timofeev, F. Schäfer, J. P. Reithmaier, T. L. Reinecke, and S. N. Walck, *Phys. Rev. Lett.* **82**, 1748 (1999).

- ⁹R. Seguin, A. Schilwa, S. Rodt, K. Pötschke, U. W. Pohl, and D. Bimberg, *Phys. Rev. Lett.* **95**, 257402 (2005).
- ¹⁰M. Abbarchi, C. A. Mastrandrea, T. Kuroda, T. Mano, K. Sakoda, N. Koguchi, S. Sanguinetti, A. Vinattieri, and M. Gurioli, *Phys. Rev. B* **78**, 125321 (2008).
- ¹¹D. Leonard, M. Krishnamurthy, C. M. Reaves, S. P. Denbaars, and P. M. Petroff, *Appl. Phys. Lett.* **63**, 3203 (1993).
- ¹²H. Yamaguchi, J. G. Belk, X. M. Zhang, J. L. Sudijono, M. R. Fahy, T. S. Jones, D. W. Pashley, and B. A. Joyce, *Phys. Rev. B* **55**, 1337 (1997).
- ¹³A. Ohtake, M. Ozeki, and J. Nakamura, *Phys. Rev. Lett.* **84**, 4665 (2000).
- ¹⁴N. Koguchi, S. Takahashi, and T. Chikyow, *J. Cryst. Growth* **111**, 688 (1991).
- ¹⁵E. Stock, T. Warming, I. Ostapenko, S. Rodt, A. Schliwa, J. A. Töfflinger, A. Lochmann, A. I. Toropov, S. A. Moshchenko, D. V. Dmitriev, V. A. Haisler, and D. Bimberg, *Appl. Phys. Lett.* **96**, 093112 (2010).
- ¹⁶T. Mano, M. Abbarchi, T. Kuroda, B. Mckimming, A. Ohtake, K. Mitsuishi, and K. Sakoda, *Appl. Phys. Express* **3**, 065203 (2010).
- ¹⁷G. Juska, V. Dimastrodonato, L. O. Mereni, A. Gocalinska, and E. Pelucchi, *Nat. Photonics* **7**, 527 (2013).
- ¹⁸T. Kuroda, T. Mano, N. Ha, H. Nakajima, H. Kumano, B. Urbaszek, M. Jo, M. Abbarchi, Y. Sakuma, K. Sakoda, I. Suemune, X. Marie, and T. Amand, *Phys. Rev. B* **88**, 041306 (2013).
- ¹⁹Y. Sakuma, M. Takeguchi, K. Takemoto, S. Hirose, T. Usuki, and N. Yokoyama, *J. Vac. Sci. Technol. B* **23**, 1741 (2005).
- ²⁰K. Takemoto, Y. Nambu, T. Miyazawa, K. Wakui, S. Hirose, T. Usuki, M. Takatsu, N. Yokoyama, K. Yoshino, A. Tomita, S. Yorozu, Y. Sakuma, and Y. Arakawa, *Appl. Phys. Express* **3**, 092802 (2010).
- ²¹X. Liu, K. Akahane, N. A. Jahan, N. Kobayashi, M. Sasaki, H. Kumano, and I. Suemune, *Appl. Phys. Lett.* **103**, 061114 (2013).
- ²²T. Mano, M. Abbarchi, T. Kuroda, C. A. Mastrandrea, A. Vinattieri, S. Sanguinetti, K. Sakodam, and M. Gurioli, *Nanotechnology* **20**, 395601 (2009).
- ²³Ch. Heyn, A. Stemman, A. Schramm, H. Welsch, and W. Hanssen, *Phys. Rev. B* **76**, 075317 (2007).
- ²⁴K. Haberern and M. D. Pashley, *Phys. Rev. B* **41**, 3226 (1990).
- ²⁵G. Gélinas, A. Lanacer, R. Leonelli, R. A. Masut, and P. J. People, *Phys. Rev. B* **81**, 235426 (2010).
- ²⁶N. A. Jahan, C. Hermannstädter, J. H. Huh, H. Sasakura, T. J. Rotter, P. Ahirwar, G. Balakrishnan, K. Akahane, M. Sasaki, H. Kumano, and I. Suemune, *J. Appl. Phys.* **113**, 033506 (2013).
- ²⁷S. Sanguinetti, M. Henini, M. G. Alessi, and M. Capizzi, *Phys. Rev. B* **60**, 8276 (1999).
- ²⁸For the single QD spectroscopy in μ PL measurement, we fabricated low QD density sample. In order to reduce the density, indium droplets were formed by a supply of 0.4 ML In at 320 °C. The other conditions were unchanged. The density of QDs is $2.6 \times 10^9 \text{ cm}^{-2}$.
- ²⁹M. Abbarchi, T. Kuroda, T. Mano, K. Sakoda, C. A. Mastrandrea, A. Vinattieri, M. Gurioli, and T. Tsuchiya, *Phys. Rev. B* **82**, 201301 (2010).
- ³⁰M. Abbarchi, T. Kuroda, T. Mano, M. Gurioli, and K. Sakoda, *Phys. Rev. B* **86**, 115330 (2012).